ACS Combinatorial Science

RESEARCH ARTICLE

pubs.acs.org/acscombsci

Combinatorial Optimization of $(Lu_{1-x}Gd_x)_3Al_5O_{12}:Ce_{3y}$ Yellow Phosphors as Precursors for Ceramic Scintillators

Xiaobin Su,[†,‡] Kong Zhang,[†,‡] Qian Liu,[†,*] Hongmei Zhong,[†] Yun Shi,[§] and Yubai Pan[§]

[†]State Key Laboratory of High Performance Ceramics and Superfine Microstructure, Shanghai Institute of Ceramics, Chinese Academy of Sciences, Shanghai 200050, China

[‡]Graduate University of the Chinese Academy of Sciences, Beijing 100049, China

[§]Key Laboratory of Transparent Opto-functional Inorganic Material, Shanghai Institute of Ceramics, Chinese Academy of Sciences, Shanghai 200050, China

Ⓢ *Supporting Information*

ABSTRACT: A combinatorial chemistry method was employed to screen the yellow phosphors of $(Lu_{1-x}Gd_x)_3Al_5O_{12}:Ce_{3y}$ as luminescenet materials. An array of 81 compositions was synthesized by inkjetting nitrate solutions into microreactor wells and sintering at high temperature. The candidate formulations were evaluated by luminescence pictures, and the optimal composition was determined to be $Lu_{2.7}Gd_{0.3}Al_5O_{12}:Ce_{0.045}$ after scale-up and detailed characterization. $Lu_{2.7}Gd_{0.3}Al_5O_{12}:Ce_{0.045}$ was also found to have a short decay time (≤53.97 ns). These results demonstrate the great potential of the $Lu_{2.7}Gd_{0.3}Al_5O_{12}:Ce_{0.045}$ as a component of ceramic scintillators.

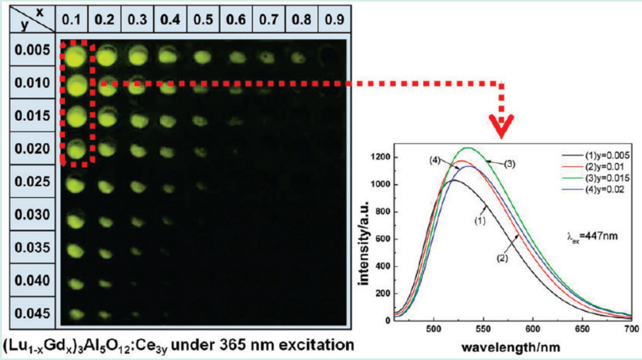

KEYWORDS: $(Lu_{1-x}Gd_x)_3Al_5O_{12}:Ce_{3y}$, combinatorial inkjetting solutions, luminescence

■ INTRODUCTION

Yttrium aluminum garnet (YAG, $Y_3Al_5O_{12}$) is a well-known inorganic compound which has excellent chemical, physical, and optical properties.[1] YAG has been widely utilized for various applications in many fields.[2] In the scintillator family, Ce-doped YAG, that is, YAG:Ce^{3+}, shows an extremely high luminescence efficiency and a short decay time.[3] Unfortunately, YAG is deficient in stopping power due to its low density (4.56 g/cm^3),[3] so isostructural LuAG:Ce ($Lu_3Al_5O_{12}$:Ce), which has a much higher density (6.695 g/cm^3),[4] is under development.[4,5] However, high-purity Lu_2O_3 powder, which is one of the starting materials of LuAG:Ce, is very expensive. It would therefore be advantageous if lower-cost elements could be found to replace Lu without sacrificing density or luminescent performance. Since the price of pure Gd_2O_3 powder is only 1/200 to 1/300 of the price of Lu_2O_3, Gd is an obvious candidate. Here, we describe a combinatorial exploration of both Gd-for-Lu replacement and Ce doping in the identification of new candidate ceramic scintillators of the general composition $(Lu_{1-x}Gd_x)_3Al_5O_{12}:Ce_{3y}$ (LuGdAG:Ce).

In analogy to previous surveys of compositions of phosphors under a variety of processing conditions,[6−8] we synthesized a 9×9 library of LuGdAG:Ce candidates using an automatic liquid injector to accurately dispense the desired components in a block array of cells. The samples were then sintered to form LuGdAG:Ce powders and evaluated by screening of luminescence intensity under UV illumination. The best compositions were synthesized on a larger scale by nitrate pyrogenation under the same experimental conditions as were used for the library preparation. The resulting powder samples were analyzed in detail to obtain their morphology, microstructure, and photoluminescence characteristics. To the best of our knowledge, this is the first report of the replacement of Gd^{3+} and the doping of Ce^{3+} ions in LuAG hosts by a combinatorial method.

■ EXPERIMENTAL PROCEDURES

The LuGdAG:Ce material libraries were prepared using a drop-on-demand inkjet delivery system (model CIJ fabricated by the University of Science and Technology of China (USTC), Hefei, China), as shown in the Supporting Information (text section and Figure S1).[6,7,9,10] Solutions of $Al(NO_3)_3\cdot 9H_2O$ (1.67 M in deionized water), $Ce(NO_3)_3\cdot 6H_2O$ (0.05 M in deionized water), Lu_2O_3 (4 N in 3 M aqueous HNO_3), and Gd_2O_3 (4 N in 3 M aqueous HNO_3) were used. Before ejection, all of the solutions were infused with argon gas for 2−3 h to expel any air dissolved in the solutions because the gas bubbles tend to

Received: October 2, 2010
Revised: October 18, 2010
Published: November 10, 2010

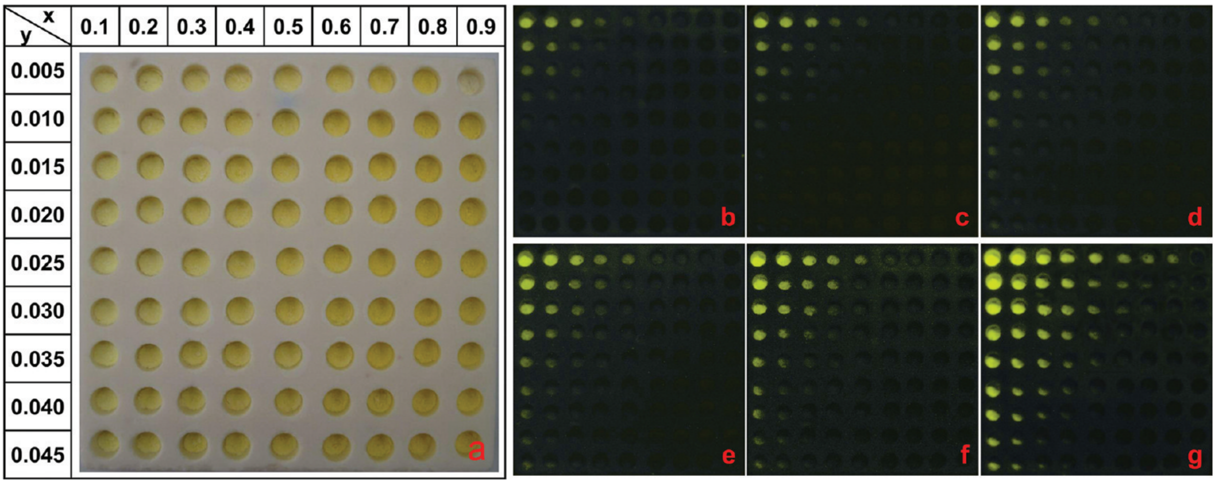

Figure 1. (a) A composition map of $(Lu_{1-x}Gd_x)_3Al_5O_{12}:Ce_{3y}$ libraries; (b−g) luminescence pictures of $(Lu_{1-x}Gd_x)_3Al_5O_{12}:Ce_{3y}$ libraries under 365 nm UV excitation, recorded by a digital camera, calcined at (b) 900, (c) 1000, (d) 1100, (e) 1200, (f) 1300, and (g) 1400 °C.

agglomerate and block the nozzle. The correct amount of each solution was deposited in each cell of an Al_2O_3 substrate according to the composition map. The substrate containing the liquid precursors was agitated in an ultrasonic bath for 6 h to mix each solution evenly and then dried at 80 °C for 24 h in an oven. The samples were then calcined at 600 °C for 4 h in a furnace at a heating rate of 4−5 °C min^{-1}. Finally, the samples were pulverized in the wells and heat-treated at various temperatures between 900 and 1400 °C in a weak reducing atmosphere produced by incomplete oxidation of activated carbon. Each plate of 81 samples was illuminated under a Hg lamp with a 365 nm broadband filter. Luminescence pictures were recorded using a 5.0 megapixel digital camera (model DiMAGE 7i, Minolta, Japan).

The three brightest luminescent samples on the recorded image were selected as the preferred compositions. These samples were independently synthesized on a larger scale by nitrate pyrogenation under the same conditions as the library's preparation for further investigation (text section S2 of the Supporting Information). The crystal structure and phase purity of the powder samples thus prepared were analyzed by X-ray diffraction (XRD) with Cu Kα radiation (λ=0.1541 nm). Scanning electron microscope (SEM) images of particle morphology were acquired on a JEOL JSM-6700F field emission scanning electron microscope. Particle sizes and shapes were observed by transmission electron microscopy (TEM, JEOL JEM2010). The excitation and emission spectra of the powders under UV light were recorded on a Hitachi F-4600 spectrometer. X-ray excited luminescence (XEL) spectra and the decay time were studied with a FLS920 fluorescence lifetime and steady state spectrometer. All measurements were performed at room temperature.

RESULTS AND DISCUSSION

The composition map and luminescent images of the $(Lu_{1-x}Gd_x)_3Al_5O_{12}:Ce_{3y}$ library under 365 nm excitation are shown in Figure 1. The 9 × 9 array consists of 81 compositions with Gd^{3+} and Ce^{3+} contents varied from x = 0.1 to 0.9 and y = 0.005 to 0.045 (Figure 1a). The images from Figure 1b−g correspond to identical libraries calcined at different temperatures, from 900 to 1400 °C. With increasing calcination temperature, the luminescence intensities of the powder samples were enhanced across the entire plate. Greater luminescence was found in the top left area of the library, with compositions of x = 0.1 and y=0.005−0.015, corresponding to lower replacement concentrations of Gd and smaller amounts of Ce doping. No significant differences in emission intensity were observed for compositions containing Gd amounts <0.1 (data not shown), so we concentrated our attention on both the replacement role of Gd^{3+} and the powder price, beginning with x=0.1.

On the basis of these combinatorial survey results, a subset of the optimal compositions were prepared through a nitrate pyrogenation reaction under the same experimental conditions as the library's preparation. The LuGdAG:Ce phase formation usually follows a two-step reaction mechanism, via pyrogenation and crystallization:

$$\text{pyrogenation}: \quad M(NO_3)_3 \rightarrow M_2O_3 + NO_x + O_2$$
$$\left(M = \left(Lu^{3+}, Gd^{3+}, Al^{3+}, Ce^{3+}\right)\right) \qquad (1)$$

$$\text{crystallization}: \quad Lu_2O_3 + Gd_2O_3 + Al_2O_3$$
$$+ Ce_2O_3 \rightarrow \text{LuGdAG : Ce} \qquad (2)$$

The normalized room temperature excitation and emission spectra of some $(Lu_{1-x}Gd_x)_3Al_5O_{12}:Ce_{3y}$ samples calcined at 1400 °C are depicted in Figure 2. All the emission spectra were recorded at λ_{ex}=447 nm, which corresponds to the excitation at the lowest energy d level of Ce^{3+}.[11] Figure 2a presents the emission spectra of $(Lu_{1-x}Gd_x)_3Al_5O_{12}:Ce_{3y}$ with a fixed Gd replacement value (x=0.1) and varied Ce^{3+} content (y=0.005, 0.01, 0.015, 0.02). The emission intensity increased with increasing Ce^{3+} content until a maximum was reached at x = 0.1 and y = 0.015. A significant red shift of the emission spectra (from 520 nm for y=0.005 to 535 nm for y=0.02) was also observed with increasing Ce^{3+} doping (Figure S2 of the Supporting Information). This red shift is in good agreement with similar findings of Bachmann et al.[11]

The corresponding excitation spectra of $(Lu_{1-x}Gd_x)_3Al_5O_{12}$: Ce_{3y} (x=0.1) are also shown in Figure 2b, taken for emission at 520 nm (y=0.005), 530 nm (y=0.01), and 535 nm (y=0.015 and 0.02), respectively. Two broad excitation bands were observed: a weak band at 348 nm and a strong band centered around 447 nm. The two excitation bands are considered to be related to the electron transition from the 4f ground state ($^2F_{5/2}$, $^2F_{7/2}$) to the

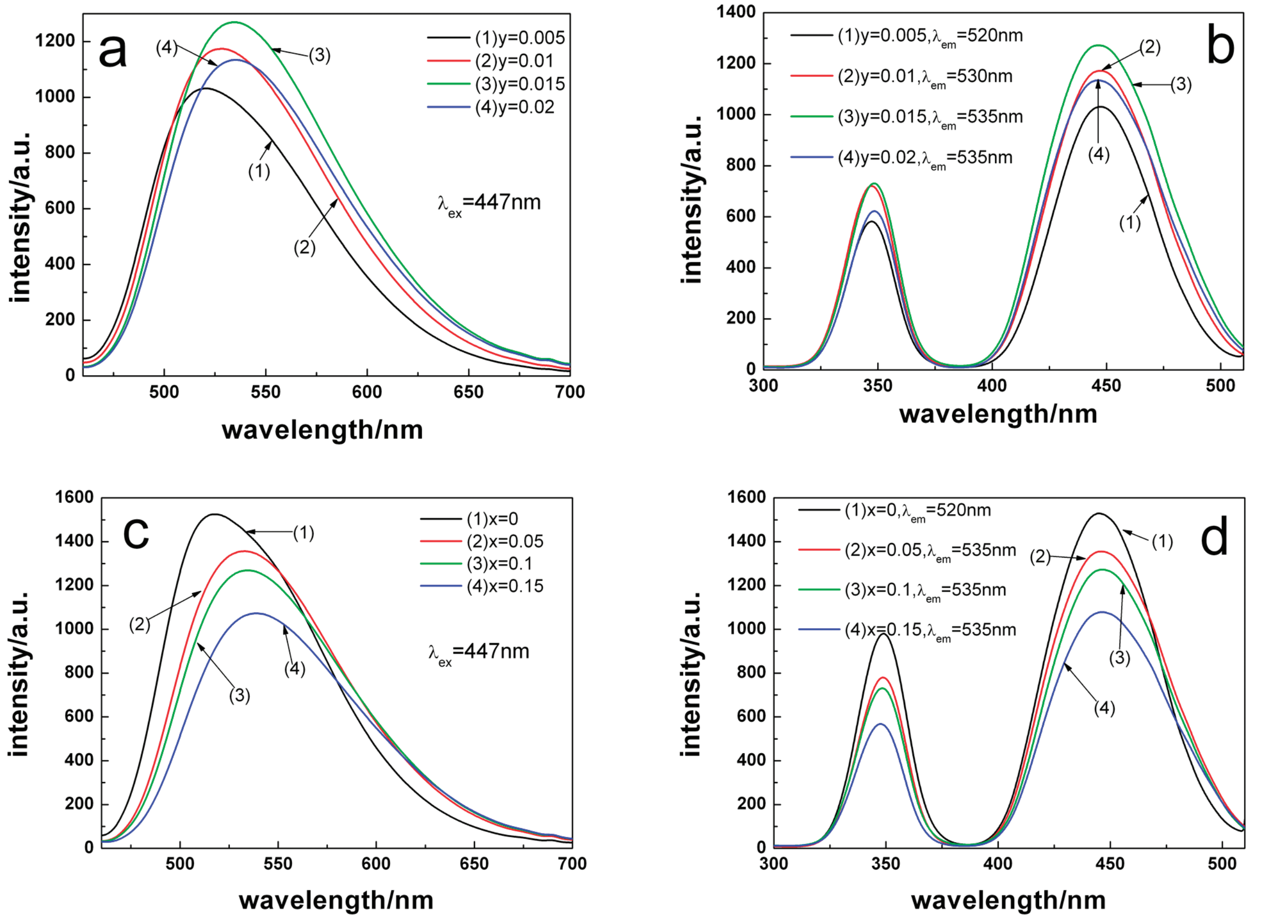

Figure 2. Excitation and emission spectra of some $(Lu_{1-x}Gd_x)_3Al_5O_{12}$:$Ce_{3y}$ powder samples. (a) Emission spectra: $x = 0.1$; $y = 0.005, 0.01, 0.015, 0.02$. (b) Excitation spectra: $x = 0.1$; $y = 0.005, 0.01, 0.015, 0.02$. (c) Emission spectra: $x = 0, 0.05, 0.1, 0.15$; $y = 0.015$. (d) Excitation spectra: $x = 0, 0.05, 0.1, 0.15$; $y = 0.015$. All powders were calcined at 1400 °C.

different crystal-field splitting levels of the 5d state of Ce^{3+}. Figure 2c presents the emission spectra of $(Lu_{1-x}Gd_x)_3Al_5O_{12}$:$Ce_{3y}$ powders with a fixed Ce composition ($y=0.015$) and varied Gd content ($x = 0, 0.05, 0.1, 0.15$). The emission intensity decreased, and the peak position shifted to the red (517 to 539 nm) with increasing of Gd^{3+} content. The red shift and emission intensity drop may result from a change in Ce^{3+} energy levels caused by the enhancement of the crystal field with increasing of Gd^{3+} content, which is expected to expand or distort the lattice cell due to the occupation of Gd^{3+} in Lu^{3+} sites ($r_{Gd^{3+}}$=1.11 Å > $r_{Lu^{3+}}$=0.92 Å). Figure 2c also shows that the intensity of emission decreases quickly at x=0.15, so x=0.1 is a better choice in terms of both cost and luminescence performance. Figure 2d depicts the relevant excitation spectra of $(Lu_{1-x}Gd_x)_3Al_5O_{12}$:$Ce_{3y}$ ($y = 0.015$). The spectra also show two bands with maxima at 348 and 447 nm. Thus, these data on scaled-up samples show $Lu_{2.7}Gd_{0.3}Al_5O_{12}$:$Ce_{0.045}$ ($x=0.1$, $y=0.015$) to be the optimum composition among those tested.

It is well-known that calcination temperature of powders is an important factor affecting crystallization and luminescence properties.[12] For the sample having the optimum composition, increasing the calcination temperature during independent scale-up syntheses provided material with greatly increased luminescence intensity, as shown in Figure 3. This indicates that the crystallization of LuGdAG:Ce powders is improved with the increase in calcination temperature.

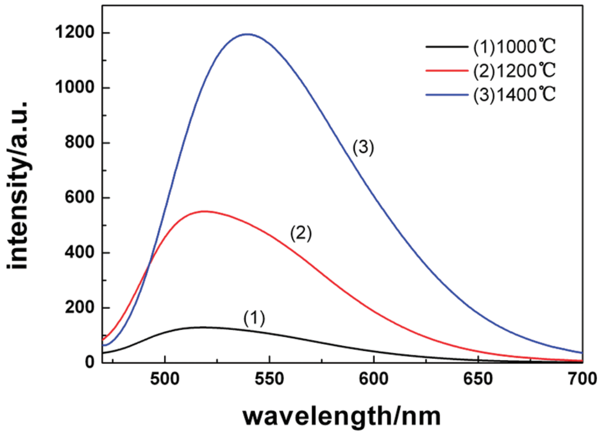

Figure 3. Emission spectra of sample $Lu_{2.7}Gd_{0.3}Al_5O_{12}$:$Ce_{0.045}$ ($x = 0.1$, $y = 0.015$), calcined at different temperatures.

Figure 4 shows the XRD results of samples of $Lu_{2.7}Gd_{0.3}Al_5O_{12}$:$Ce_{0.045}$ ($x=0.1$, $y=0.015$), calcined at different temperatures for 2 h in a weak reducing atmosphere. The theoretical patterns for LuAG and GAG are also shown in Figure 4a and b. These data show that a pure garnet structure was obtained by calcinations above 900 °C. No other phase is present by comparison with standard X-ray diffraction patterns. The fwhm

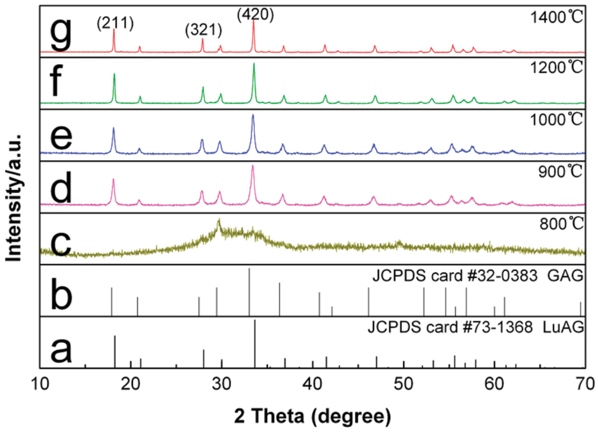

Figure 4. XRD results of sample $Lu_{2.7}Gd_{0.3}Al_5O_{12}$:$Ce_{0.045}$ ($x = 0.1$, $y = 0.015$) calcined at different temperatures.

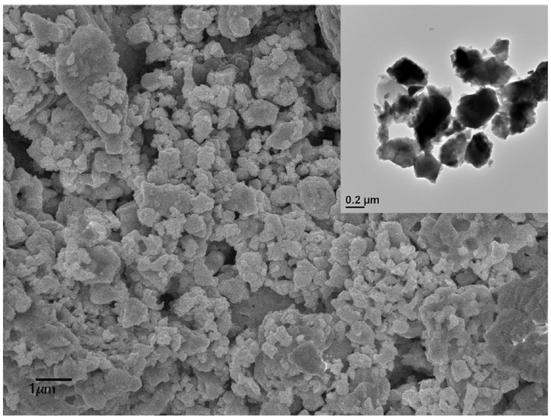

Figure 5. SEM image for sample $Lu_{2.7}Gd_{0.3}Al_5O_{12}$:$Ce_{0.045}$. The inset is the TEM image with higher resolution.

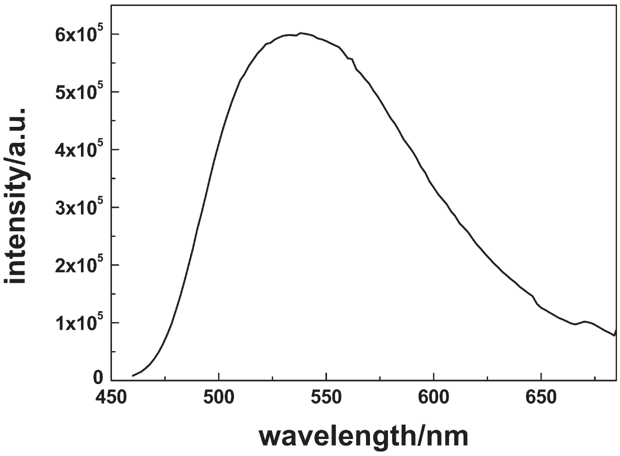

Figure 6. XEL spectrum for sample $Lu_{2.7}Gd_{0.3}Al_5O_{12}$:$Ce_{0.045}$ ($x = 0.1$, $y = 0.015$) calcined at 1400 °C.

(full width at half-maximum) values of diffraction peaks of the (420) plane decreased for the powders calcined at higher temperatures, from 0.369 for 900 °C calcination to 0.131 for 1400 °C calcination (Figure S3 of the Supporting Information), also supporting the conclusion that crystallization is enhanced by the increase in temperature. SEM and TEM of $Lu_{2.7}Gd_{0.3}Al_5O_{12}$:$Ce_{0.045}$ powder, heat-treated at 1400 °C for 2 h, showed many large agglomerated particles (200−400 nm in diameter) composed of smaller particles (Figure 5).

XEL analysis of this material is shown in Figure 6 to aid in the evaluation of scintillation efficiency. No obvious difference was noted in the peak shape and position of the emission spectra under X-ray or UV excitation. The photoluminescence decay time for 5d → 4f transition of Ce^{3+} in the $Lu_{2.7}Gd_{0.3}Al_5O_{12}$:$Ce_{0.045}$ sample at room temperature was also measured (Figure S4 of Supporting Information). The data were fit to a fast decay time of ∼17.95 ns, contributed mainly by Ce^{3+} on the particle surface and accounting for only 14.35% of the response, and a slow decay time of ∼53.97 ns caused by Ce^{3+} in the bulk phase and playing the dominant role. These scintillation characterizations suggest that the optimal composition $Lu_{2.7}Gd_{0.3}Al_5O_{12}$:$Ce_{0.045}$ could be a good candidate for a starting powder for scintillators with a shorter decay time, an application that we will pursue in the future.

CONCLUSION

In summary, combinatorial libraries of yellow phosphors $(Lu_{1-x}Gd_x)_3Al_5O_{12}$:$Ce_{3y}$ were synthesized and screened for luminescence intensity. Scaled-up synthesis and characterization showed that the optimum composition was $Lu_{2.7}Gd_{0.3}Al_5O_{12}$:$Ce_{0.045}$, having a strong yellow emission under either X-ray or UV excitation. The powders had a fast decay time of 17.95 ns (14.35%), and a slow decay time of 53.97 ns (85.65%). On the basis of these results, it is reasonable to believe that a lower-Gd-replaced LuGdAG:Ce composition could be potentially used for the application in scintillators in consideration of cost and luminescence performance.

ASSOCIATED CONTENT

Ⓢ **Supporting Information.** Details about the drop-on-demand inkjet delivery system (text S1), scaled-up nitrate pyrogenation procedure (text S2), and Figures S1−S4. This information is available free of charge via the Internet at http://pubs.acs.org/.

AUTHOR INFORMATION

Corresponding Author

*Phone: +86 021 52412612. Fax: +86 021 52413122. E-mail: qianliu@sunm.shcnc.ac.cn.

ACKNOWLEDGMENT

This work was supported by the National High Technology Research and Development Program of China (863 Program, no. 2009AA03Z437) and the Science and Technology Commission of Shanghai Municipality.

REFERENCES

(1) Zhou, S. H.; Fu, Z. L.; Zhang, J. J.; Zhang, S. Y. Spectral properties of rare-earth ions in nanocrystalline YAG:Re (Re = Ce^{3+}, Pr^{3+}, Tb^{3+}). *J. Lumin.* **2006,** *118,* 179–185.

(2) Kaithwas, N.; Deshmukh, M.; Kar, S.; Dave, M.; Lalla, N. P.; Ryu, H.; Bartwal, K. S. Preparation Of $Y_3Al_5O_{12}$ nanocrystals by low temperature glycol route. *Cryst. Res. Technol.* **2007,** *42,* 991–994.

(3) Wang, Z. F.; Xu, M.; Zhang, W. P.; Yin, M. Synthesis and luminescent properties of nano-scale LuAG:RE^{3+} (Ce, Eu) phosphors prepared by co-precipitation method. *J. Lumin.* **2007**, *122*, 437–439.

(4) Blazek, K.; Krasnikov, A.; Nejezchleb, K.; Nikl, M.; Savikhina, T.; Zazubovich, S. Luminescence and defects creation in Ce^{3+}-doped $Lu_3Al_5O_{12}$ crystals. *Phys. Status Solidi B* **2004**, *241*, 1134–1140.

(5) Nikl, M.; Mihokova, E.; Mares, J. A.; Vedda, A.; Martini, M.; Nejezchleb, K.; Blazek, K. Traps and timing characteristics of LuAG: Ce^{3+} scintillator. *Phys. Status Solidi A* **2000**, *181*, R10–R12.

(6) Chan, T. S.; Liu, Y. M.; Liu, R. S. Combinatorial search for green and blue phosphors of high thermal stabilities under UV excitation based on the $K(Sr_{1-x-y})PO_4:Tb_x^{3+}Eu_y^{2+}$ System. *J. Comb. Chem.* **2008**, *10*, 847–850.

(7) Chen, L.; Bao, J.; Gao, C. Combinatorial synthesis of insoluble oxide library from ultrafine/nano particle suspension using a drop-on-demand inkjet delivery system. *J. Comb. Chem.* **2004**, *6*, 699–702.

(8) Sohn, K. S.; Park, D. H.; Cho, S. H.; Kwak, J. S.; Kim, J. S. Computational evolutionary optimization of red phosphor for use in tricolor white LEDs. *Chem. Mater.* **2006**, *18*, 1768–1772.

(9) Chen, L.; Fu, Y. B.; Zhang, G. B.; Bao, J.; Gao, C. Optimization of Pr^{3+}, Tb^{3+}, and Sm^{3+} co-doped $(Y_{0.65}Gd_{0.35})BO_3:Eu_{0.05}^{3+}$ VUV phosphors through combinatorial approach. *J. Comb. Chem.* **2008**, *10*, 401–404.

(10) Chan, T. S.; Kang, C. C.; Liu, R. S.; Chen, L.; Liu, X. N.; Ding, J. J.; Bao, J.; Gao, C. Combinatorial study of the optimization of Y_2O_3:Bi, Eu red phosphors. *J. Comb. Chem.* **2007**, *9*, 343–346.

(11) Bachmann, V.; Ronda, C.; Meijerink, A. Temperature quenching of yellow Ce^{3+} luminescence in YAG:Ce. *Chem. Mater.* **2009**, *21*, 2077–2084.

(12) Pan, Y. X.; Wu, M. M.; Su, Q. Comparative investigation on synthesis and photoluminescence of YAG:Ce phosphor. *Mater. Sci. Eng., B* **2004**, *106*, 251–256.